

Supplementary Information

Off-the-shelf thermosalience of anthracene-9-thiocarboxamide

Gary C. George III,^a Samantha J. Kruse,^b Tori Z. Forbes^b and Kristin M. Hutchins^{*a,c}

^a Department of Chemistry, University of Missouri, 601 S College Avenue, Columbia, MO 65211, USA. Email: kristin.hutchins@missouri.edu

^b Department of Chemistry, University of Iowa, Chemistry Building, Iowa City, IA 52242, USA.

^c MU Materials Science & Engineering Institute, University of Missouri, Columbia, MO 65211

1. Materials and Crystallization	S2
2. X-ray Diffraction Information and Data Tables	S3-S6
3. Thermal Expansion Data and Intermolecular Interaction Distances	S7-S8
4. Variation of the Unit Cell Parameters	S9-S10
5. Expansivity Indicatrix Diagram	S11-S12
6. Additional Crystal Structure Images	S13-S14
7. Differential Scanning Calorimetry (DSC)	S15-S16
8. Powder X-ray Diffraction (PXRD) Data	S17-S18
9. Optical Microscopy with Variable-Temperature Stage	S19
10. References	S20

1. Materials and Crystallization

Materials

Anthracene-9-thiocarboxamide (AnThio) was purchased from Oakwood Chemicals. Ethyl acetate was purchased from Fisher Chemicals. The commercially obtained AnThio was crystalline but was twinned. Recrystallization from ethyl acetate afforded crystals of the same unit cell suitable for variable-temperature single-crystal X-ray diffraction data collection.

Crystallization

All crystallization experiments were conducted at ambient temperature and humidity. After dissolving the solid in ethyl acetate using a short period of heating, the vials were left at room temperature and ethyl acetate was allowed to slowly evaporate (ca. 3 days). The samples were kept from light (using aluminium foil or placing in an opaque container) to avoid possible photodimerization.

2. X-ray Diffraction Information and Data Tables

Data were collected on a Rigaku XtaLAB Synergy- κ diffractometer equipped with a PhotonJet- i X-ray source operated at 50 W (50 kV, 1 mA) to generate Cu K α radiation ($\lambda = 1.54178 \text{ \AA}$), or Mo K α radiation ($\lambda = 0.71073 \text{ \AA}$) and a HyPix-6000HE HPC (hybrid photon counting) detector. Crystals were transferred from the vial and placed on a glass slide in type NVH immersion oil by Cargille. A Zeiss Stemi 305 microscope was used to identify a suitable specimen for X-ray diffraction from a representative sample of the material. The crystal and a small amount of the oil were collected on a 50 micron MiTeGen cryoloop and transferred to the instrument where it was placed under a cold nitrogen stream (Oxford). Data were collected at temperatures of 300 K,¹ 280 K, 260 K, 240 K, 220 K, 200 K, 180 K, 160 K, 140 K, 120 K, and 100 K with a transition rate of 2 K/minute between the temperatures. The data collected between 140-100 K was poor due to the crystal fragmenting during thermosalience. The sample was optically centered with the aid of a video camera to ensure that no translations were observed as the crystal was rotated through all positions. The crystal was measured for size, morphology, and color.

After data collection, the unit cell was re-determined using a subset of the full data collection for each temperature. Intensity data were corrected for Lorentz, polarization, and background effects using *CrysAlis^{Pro}*.² A numerical absorption correction was applied based on a Gaussian integration over a multifaceted crystal and followed by a semi-empirical correction for adsorption applied using the program *SCALE3 ABSPACK*.³ The program *SHELXT*⁴ was used for the initial structure solution and *SHELXL*⁵ was used for the refinement of the structures. Both of these programs were utilized within the *OLEX2*⁶ software. Hydrogen atoms bound to carbon atoms were located in the difference Fourier map and were geometrically constrained using the appropriate AFIX commands.

The structure contained a small amount of disorder in the anthracene molecule that contained S1. Upon modelling this disorder, it was found to be partially cyclized via a solid-state [4+4] cycloaddition reaction. Throughout the temperature range studied, the disorder was consistent, ranging from 4 - 5%. The disorder was omitted since it was a low percentage, and modelling did not significantly improve the statistical parameters. Additional single crystals of AnThio containing a higher percentage of the same disorder (ca. 9%) also exhibited thermosalience in the same temperature range. The disorder also remained nearly constant with respect to temperature in this crystal.

An attempt was made to characterize the low temperature phase by mounting the crystal on a glass fiber with epoxy. The epoxy was allowed to harden, and the crystal was mounted at 200 K and cooled to 100 K with a transition rate of 2 K/min. The crystal was occasionally screened while the temperature was decreasing to make sure crystallinity and diffraction capability persisted. Once reaching 100 K, data was collected, and it was found to be of very poor quality. Approximately 60% of the reflections could be indexed to the original high temperature phase unit cell; however, the R_{int} was much above what is reasonably considered publishable.

Table S1. X-ray data for AnThio at 280, 260, and 240 K.

compound formula	C ₁₅ H ₁₁ NS	C ₁₅ H ₁₁ NS	C ₁₅ H ₁₁ NS
formula mass	237.31	237.31	237.31
crystal system	Triclinic	Triclinic	Triclinic
space group	<i>P</i> -1	<i>P</i> -1	<i>P</i> -1
a/Å	9.2758(2)	9.2540(2)	9.2356(2)
b/Å	9.9051(2)	9.9104(2)	9.9171(2)
c/Å	13.2567(3)	13.2402(3)	13.2232(3)
α /°	82.254(2)	82.185(2)	82.118(2)
β /°	83.462(2)	83.436(2)	83.407(2)
γ /°	77.9570(10)	77.9410(10)	77.9230(10)
V/Å ³	1175.69(4)	1171.81(4)	1168.48(4)
ρ_{calc} /g cm ⁻³	1.341	1.345	1.349
T/K	279.95(10)	259.95(10)	239.95(10)
Z	4	4	4
radiation type	CuK α	CuK α	CuK α
absorption coefficient, μ /mm ⁻¹	2.211	2.218	2.225
crystal size/mm ³	0.320 x 0.185 x 0.086	0.320 x 0.185 x 0.086	0.320 x 0.185 x 0.086
no. of reflections measured	20936	21294	21945
no. of independent reflections	4677	4668	4654
no. of reflection ($I > 2\sigma(I)$)	3967	3997	4083
R _{int}	0.0726	0.0712	0.0705
R ₁ ($I > 2\sigma(I)$)	0.0458	0.0470	0.0501
wR(F ²) ($I > 2\sigma(I)$)	0.1215	0.1252	0.1360
R ₁ (all data)	0.0539	0.0551	0.0561
wR(F ²) (all data)	0.1277	0.1320	0.1404
Goodness-of-fit	1.033	1.023	1.063
CCDC deposition number	2347862	2347863	2347864

Table S2. X-ray data for AnThio at 220, 200, 180, and 160 K.

compound formula	C ₁₅ H ₁₁ NS	C ₁₅ H ₁₁ NS	C ₁₅ H ₁₁ NS	C ₁₅ H ₁₁ NS
formula mass	237.31	237.31	237.31	237.31
crystal system	Triclinic	Triclinic	Triclinic	Triclinic
space group	<i>P</i> -1	<i>P</i> -1	<i>P</i> -1	<i>P</i> -1
<i>a</i> /Å	9.2177(2)	9.20120(10)	9.18680(10)	9.17430(10)
<i>b</i> /Å	9.9216(2)	9.9272(2)	9.92770(10)	9.9298(2)
<i>c</i> /Å	13.2043(3)	13.1869(2)	13.1688(2)	13.1500(2)
α /°	82.062(2)	82.0090(10)	81.9520(10)	81.9170(10)
β /°	83.369(2)	83.3400(10)	83.3050(10)	83.2870(10)
γ /°	77.9280(10)	77.9210(10)	77.9300(10)	77.9370(10)
<i>V</i> /Å ³	1164.89(4)	1161.71(3)	1158.19(3)	1155.11(3)
ρ_{calc} /g cm ⁻³	1.353	1.357	1.361	1.365
T/K	219.95(10)	199.95(10)	179.94(10)	159.92(13)
<i>Z</i>	4	4	4	4
radiation type	CuK α	CuK α	CuK α	CuK α
absorption coefficient, μ /mm ⁻¹	2.232	2.238	2.244	2.250
crystal size/mm ³	0.320 x 0.185 x 0.086	0.320 x 0.185 x 0.086	0.320 x 0.185 x 0.086	0.320 x 0.185 x 0.086
no. of reflections measured	22601	23617	24546	25248
no. of independent reflections	4629	4616	4602	4592
no. of reflection (<i>I</i> > 2 σ (<i>I</i>))	4108	4181	4227	4226
<i>R</i> _{int}	0.0725	0.0714	0.0717	0.0720
<i>R</i> ₁ (<i>I</i> > 2 σ (<i>I</i>))	0.0512	0.0519	0.0516	0.0508
w <i>R</i> (<i>F</i> ²) (<i>I</i> > 2 σ (<i>I</i>))	0.1385	0.1411	0.1371	0.1342
<i>R</i> ₁ (all data)	0.0566	0.0562	0.0552	0.0540
w <i>R</i> (<i>F</i> ²) (all data)	0.1431	0.1380	0.1399	0.1367
Goodness-of-fit	1.062	1.062	1.064	1.056
CCDC deposition number	2347865	2347866	2347867	2347868

3. Thermal Expansion Data and Intermolecular Interaction Distances

The TE coefficients were calculated using the PASCAL program.⁷ The unit cell parameters from the crystallographic data sets collected from 300 – 160 K were used for the TE calculations.

Table S3. TE coefficients for AnThio over different temperature ranges. Errors are denoted in parentheses, and the approximate crystallographic axes are denoted in brackets.

Temperature range	α_{x_1} (MK ⁻¹) [axis]	α_{x_2} (MK ⁻¹) [axis]	α_{x_3} (MK ⁻¹) [axis]	α_V (MK ⁻¹)
160-300 K	-27 (2) [-1 7 1]	74 (1) [3 -1 2]	102 (3) [5 1 -3]	151 (2)
240-300 K	-34 (1) [0 4 1]	72 (1) [1 -2 4]	120 (3) [4 0 -1]	159 (3)
160-220 K	-17 (2) [-1 7 1]	69 (1) [6 -1 2]	90 (1) [-3 -1 4]	142 (1)

Table S4. Intermolecular interaction distances that contribute to the TE in AnThio.

N-H...S (Å) 300 K	N-H...S (Å) 160 K	Δ (Å)
3.393	3.361	0.032
3.404	3.377	0.027

C-H...S (Å) 300 K	C-H...S (Å) 160 K	Δ (Å)
3.917	3.876	0.041
3.848	3.802	0.046
3.806	3.768	0.038
3.962	3.912	0.050
3.850	3.798	0.052
3.793	3.757	0.036
		Avg: 0.044

N-H... π (Å) 300 K	N-H... π (Å) 160 K	Δ (Å)
3.515	3.488	0.027
3.442	3.414	0.028
3.557	3.521	0.036
3.520	3.517	0.003
3.566	3.533	0.033
		Avg: 0.025

C-H...C-H (Å) 300 K	C-H...C-H (Å) 160 K	Δ (Å)
3.720	3.682	0.038

$\pi \cdots \pi$ (Å) 290 K	$\pi \cdots \pi$ (Å) 190 K	Δ (Å)
3.790	3.754	0.036
3.710	3.676	0.034
3.768	3.725	0.043
3.685	3.640	0.045
		Avg: 0.040

4. Variation of the Unit Cell Parameters

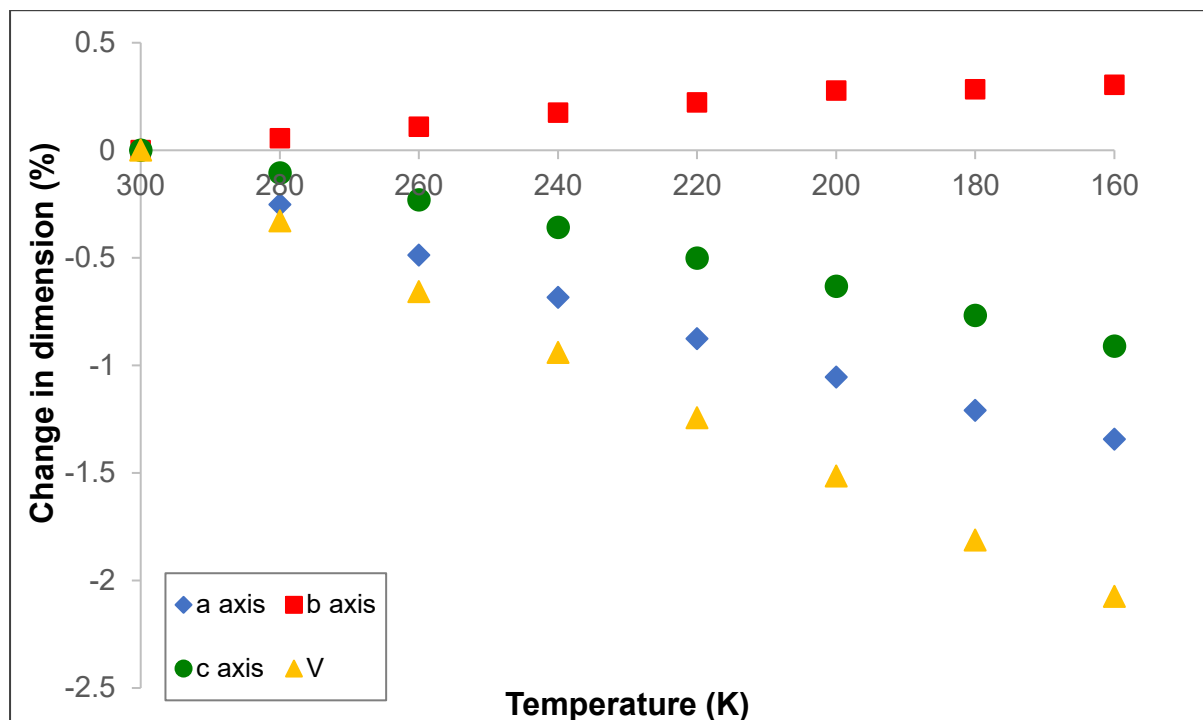


Figure S1. Percent change in unit cell dimension (length or volume) as a function of temperature for AnThio from 300 – 160 K. All values are relative to the unit cell at 300 K.

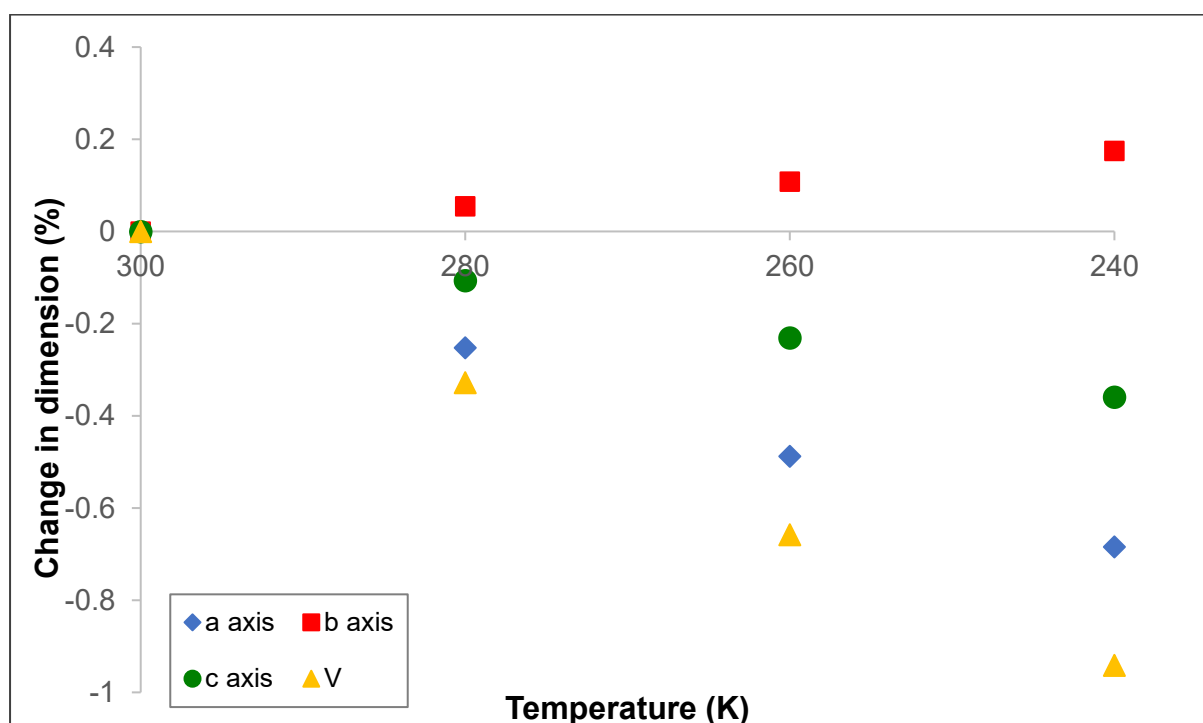


Figure S2. Percent change in unit cell dimension (length or volume) as a function of temperature for AnThio from 300 – 240 K. All values are relative to the unit cell at 300 K.

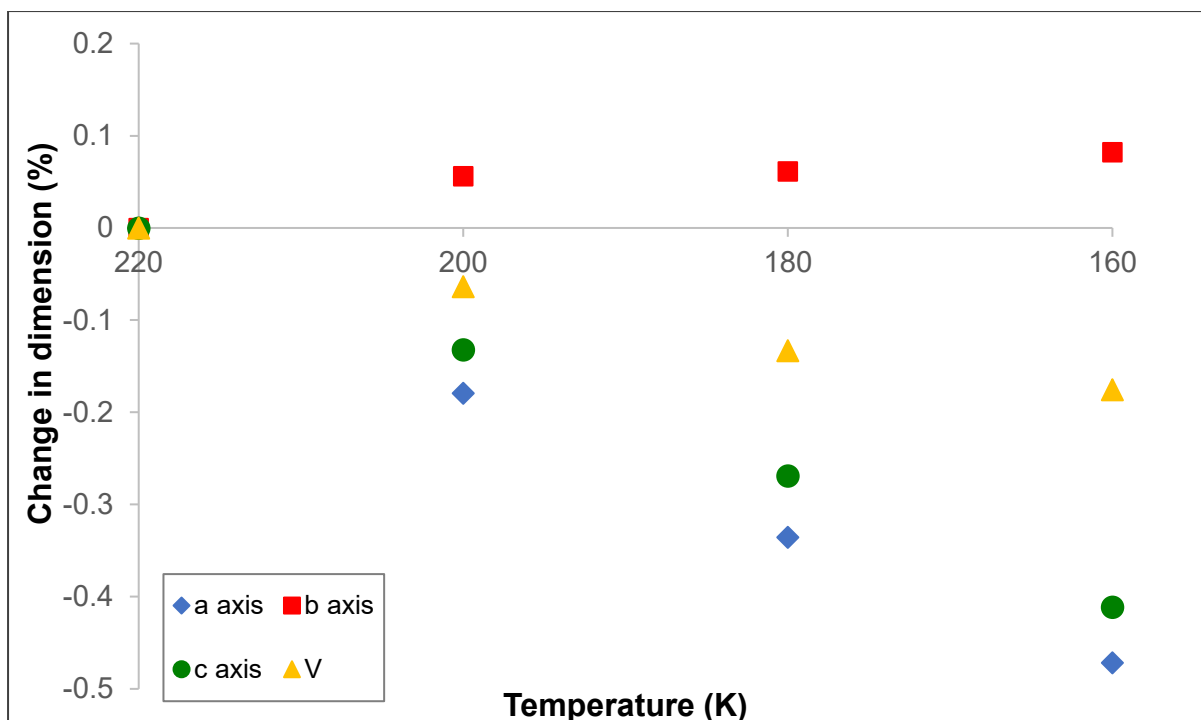


Figure S3. Percent change in unit cell dimension (length or volume) as a function of temperature for AnThio from 220 – 160 K. All values are relative to the unit cell at 220 K.

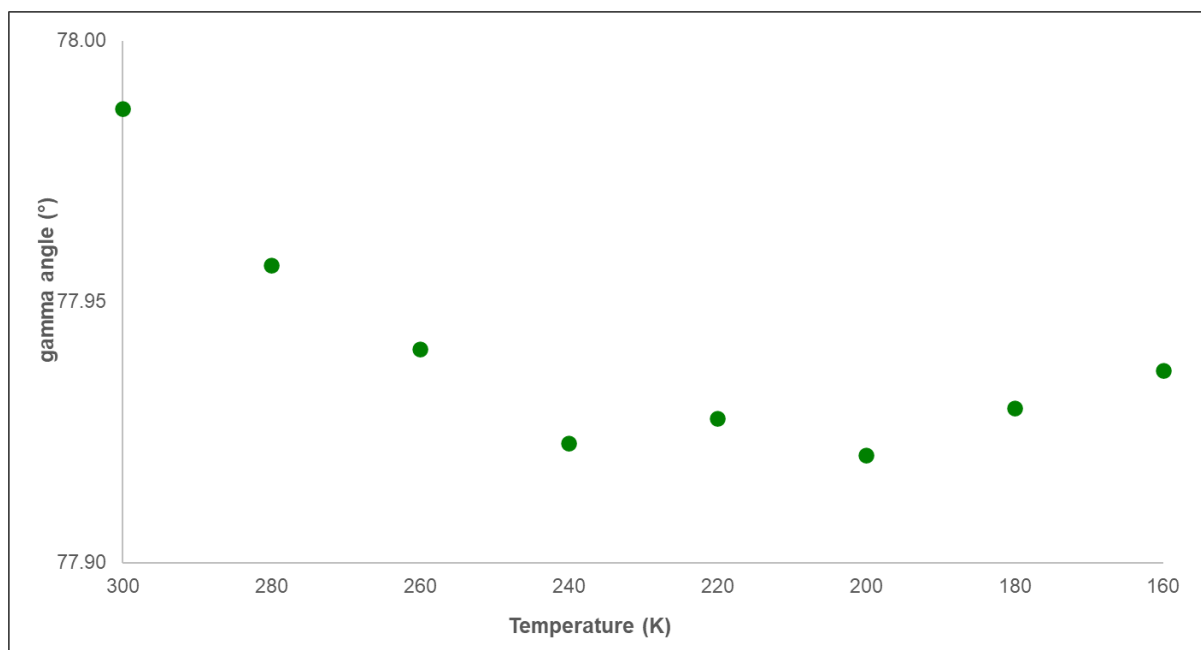


Figure S4. Change in γ angle of AnThio as a function of temperature from 300 – 160 K.

5. Expansivity Indicatrix Diagrams

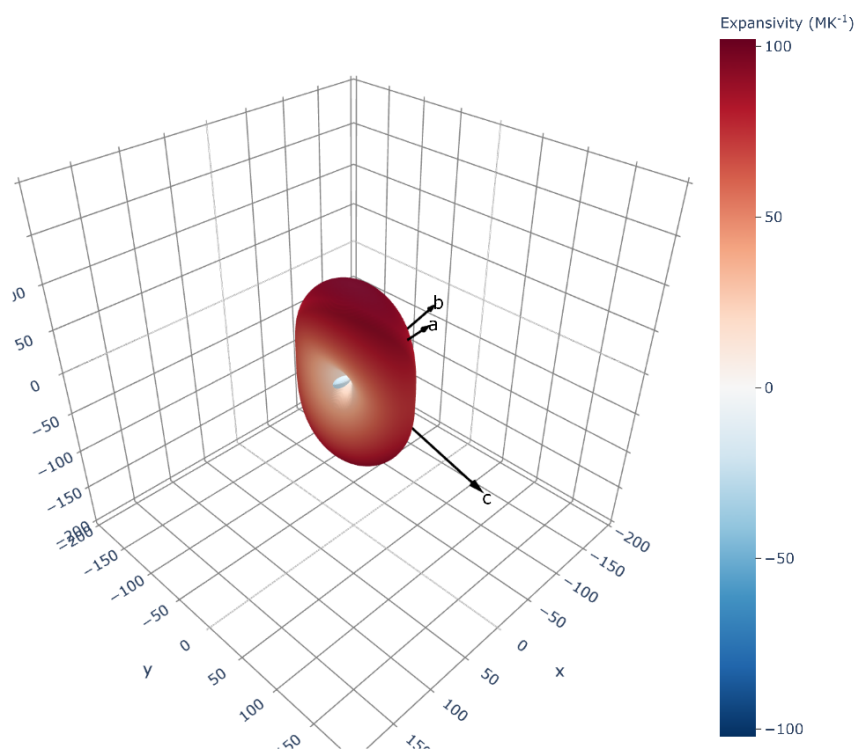


Figure S5. Thermal expansivity indicatrix from 160 – 300 K for AnThio.

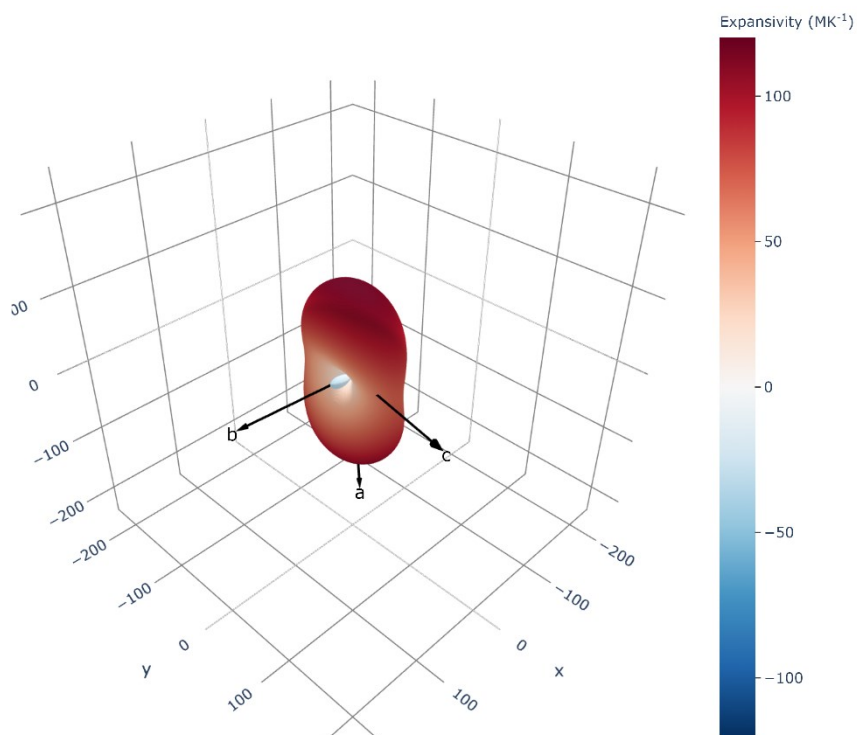


Figure S6. Thermal expansivity indicatrix from 240 – 300 K for AnThio.

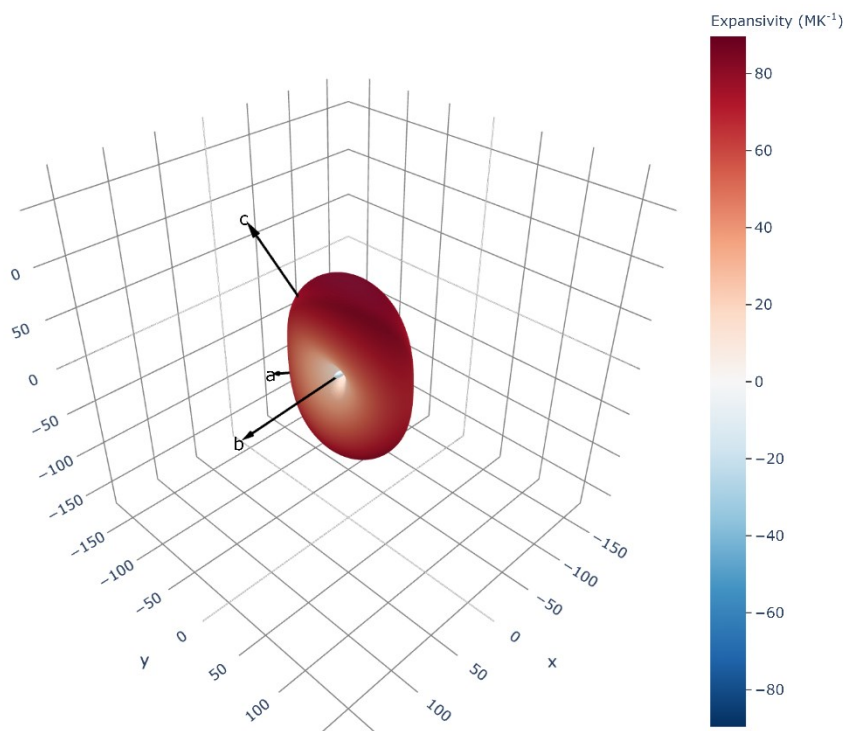


Figure S7. Thermal expansivity indicatrix from 160 – 220 K for AnThio.

6. Additional Crystal Structure Images

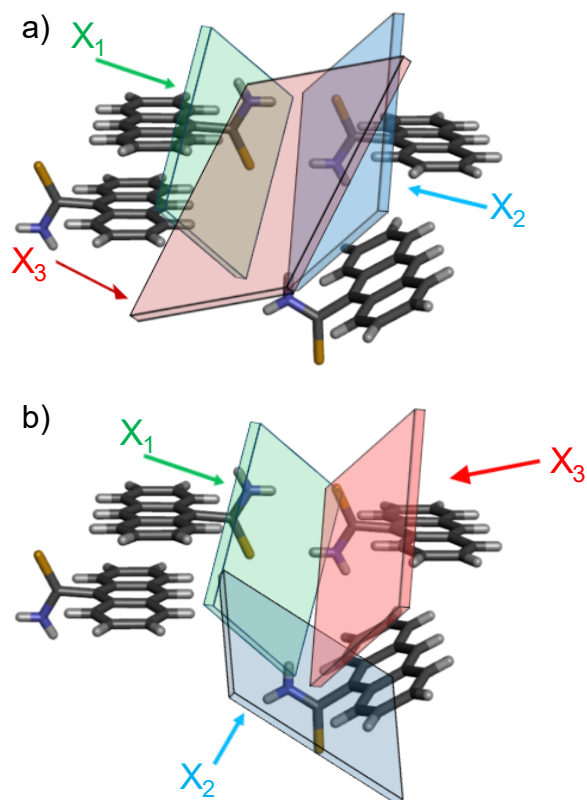


Figure S8. Planes and arrows highlighting the directions of TE, along with the switching of the X₂ and X₃ directions between a) 160 – 220 K and b) 240 – 300 K. Green corresponds to X₁, blue corresponds to X₂, and red corresponds to X₃.

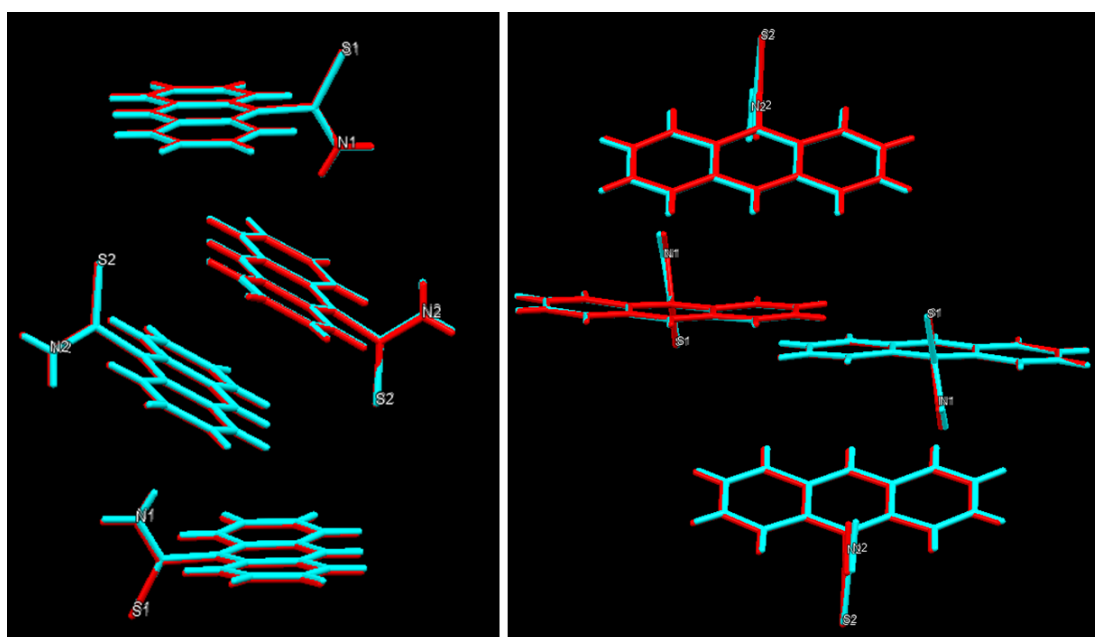


Figure S9. Overlay of crystal packing of AnThio at 300 K (red) and 160 K (cyan).

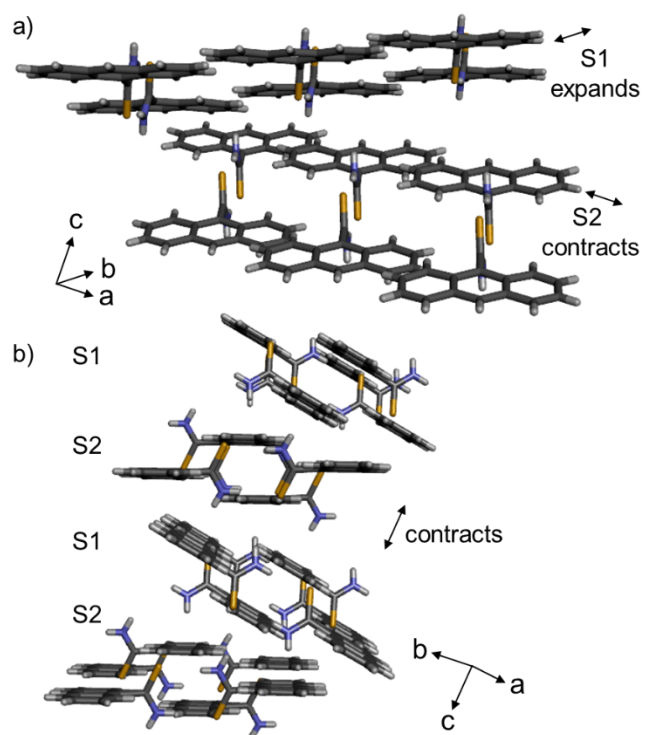


Figure S10. X-ray crystal structures of AnThio showing a) simultaneous expansion and contraction of neighboring moieties and b) overall contraction in the π -stacked direction. AnThio molecules containing S1 or S2 are labeled. The behavior of AnThio upon cooling is highlighted with the text and two-sided arrows.

7. Differential Scanning Calorimetry (DSC)

DSC data was collected on a DSC Q100 by TA Instruments using a hermetically sealed pan. The sample was cooled from room temperature to $-150\text{ }^{\circ}\text{C}$ using a cooling rate of $5\text{ }^{\circ}\text{C}/\text{min}$. For the cycle experiments, the cooling was followed by warming the sample from $-150\text{ }^{\circ}\text{C}$ to room temperature using a heating rate of $5\text{ }^{\circ}\text{C}/\text{min}$.

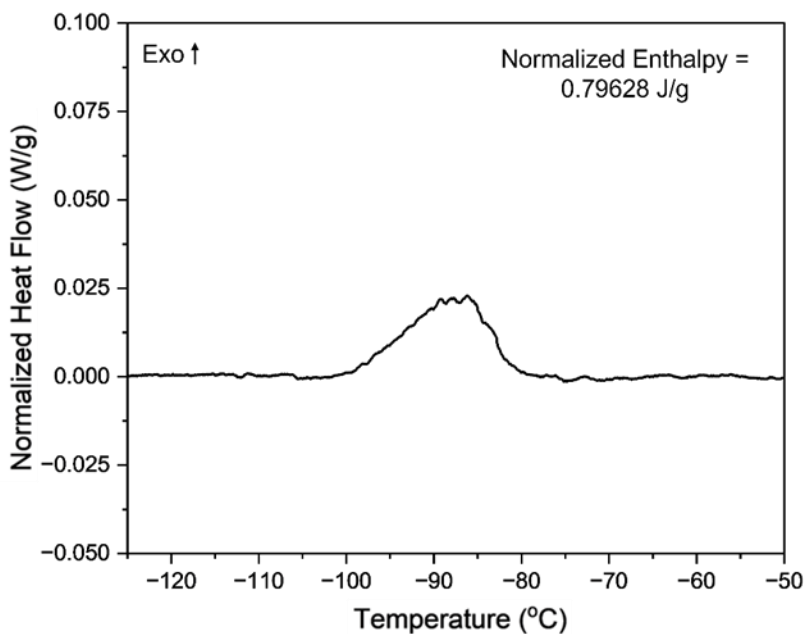


Figure S11. DSC thermograph of AnThio from the manufacturer's bottle showing thermosaliency at $-86\text{ }^{\circ}\text{C}$ (187 K). The overall enthalpy is noted on the plot.

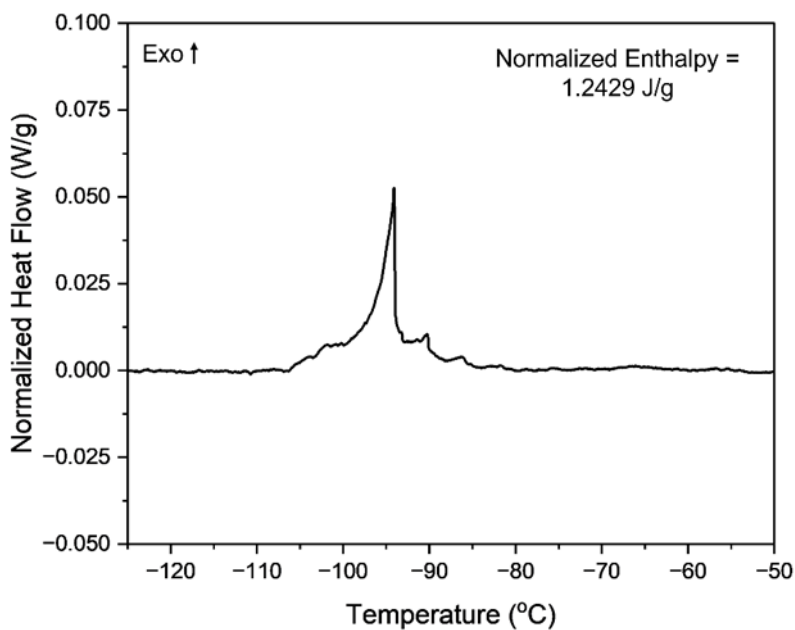


Figure S12. DSC thermograph of AnThio after recrystallization from ethyl acetate. The sharp peak is at $-94\text{ }^{\circ}\text{C}$ (179 K). The overall enthalpy is noted on the plot.

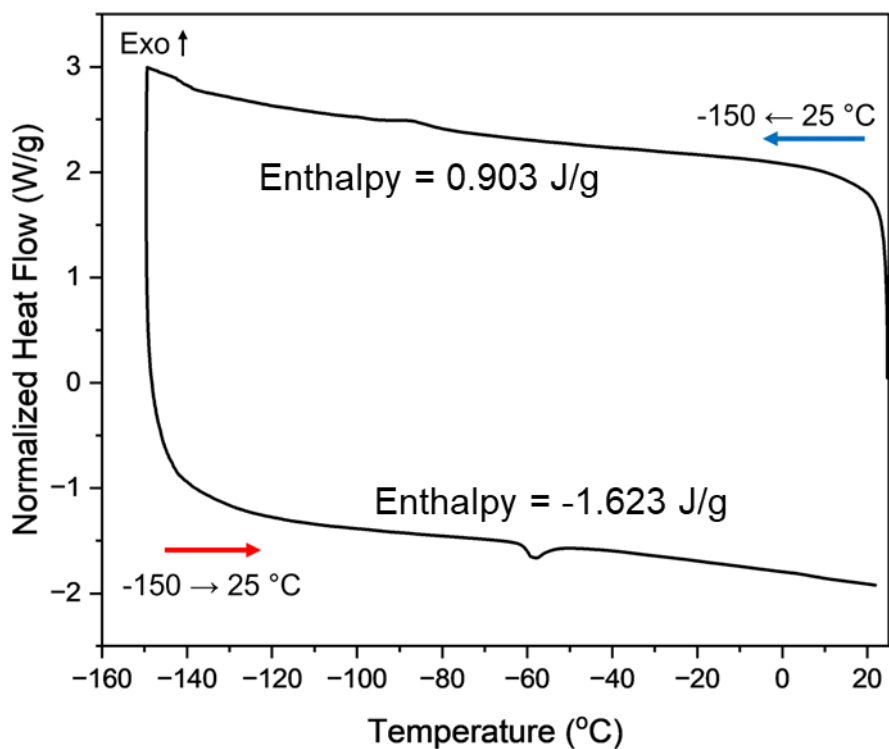


Figure S13. DSC thermogram of AnThio from the manufacturer's bottle. The peak on cooling is at $-88\text{ }^{\circ}\text{C}$ (185 K), and the peak on heating is at $-59\text{ }^{\circ}\text{C}$ (214 K). The overall enthalpy values are noted on the plot.

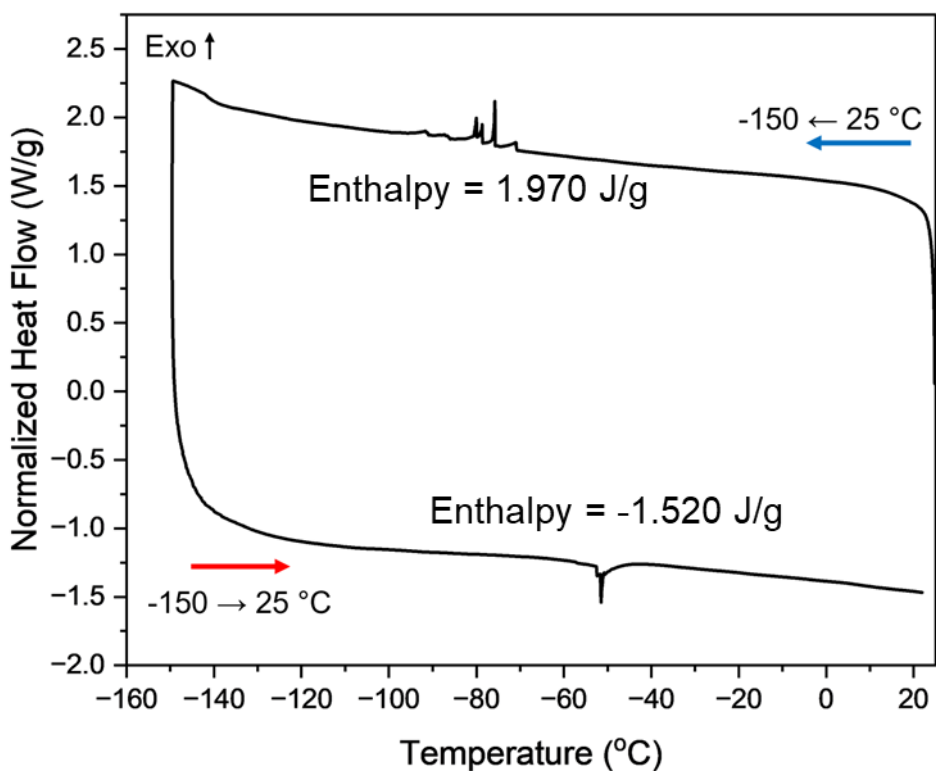


Figure S14. DSC thermogram of AnThio after recrystallization from ethyl acetate. The sharp peak upon cooling is at $-76\text{ }^{\circ}\text{C}$ (197 K), and the sharp peak upon heating is at $-52\text{ }^{\circ}\text{C}$ (221 K). The overall enthalpy values are noted on the plot.

8. Powder X-ray Diffraction (PXRD) Data

Diffraction patterns for the low temperature phase were collected on a high-resolution laboratory Stoe Stadi-P powder diffractometer, operating in Debye-Scherrer (transmission) geometry. The diffractometer was equipped with a molybdenum X-ray source, and monochromatic Mo-K α_1 radiation was obtained by a primary Ge(111) monochromator (centered at 0.7093 Å). Scattered X-ray intensity was simultaneously collected by two highly sensitive, linearly positioned silicon-strip (Mythen Dectris 1K) detectors. Sample preparation involved very gentle grinding of the materials with a mortar and pestle and packing in borosilicate capillaries with a 0.7 mm diameter. During measurements, the capillary was rotated for improved particle statistics. Diffraction data was collected at -100 °C (173 K) using an Oxford cryosystem.

Diffraction patterns for the room temperature phase were collected on a Rigaku MiniFlex II powder diffractometer. An X-ray diffraction pattern was obtained by scanning a 2θ range of 5-50°, step size = 0.02°, and scan time of 5°/minute. The X-ray source was Cu K α radiation ($\lambda = 1.5418$ Å) with an anode voltage of 30 kV and a current of 15 mA. Diffraction intensities were recorded on a position sensitive detector (D/teX Ultra). The sample was prepared as a standard powder mount.

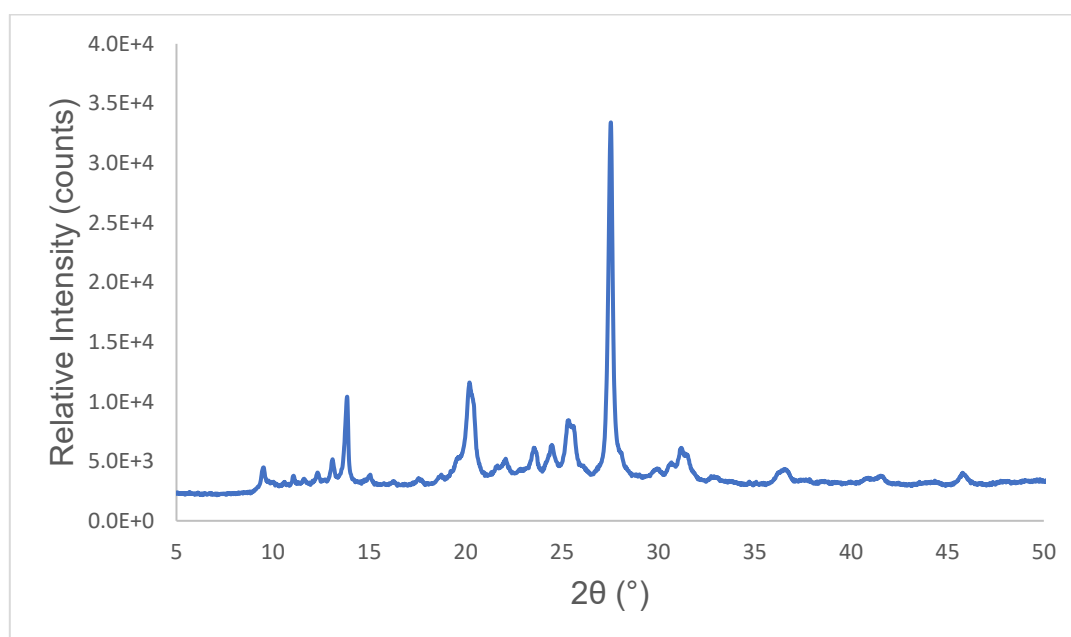


Figure S15. PXRD pattern of AnThio at room temperature after recrystallization from ethyl acetate.

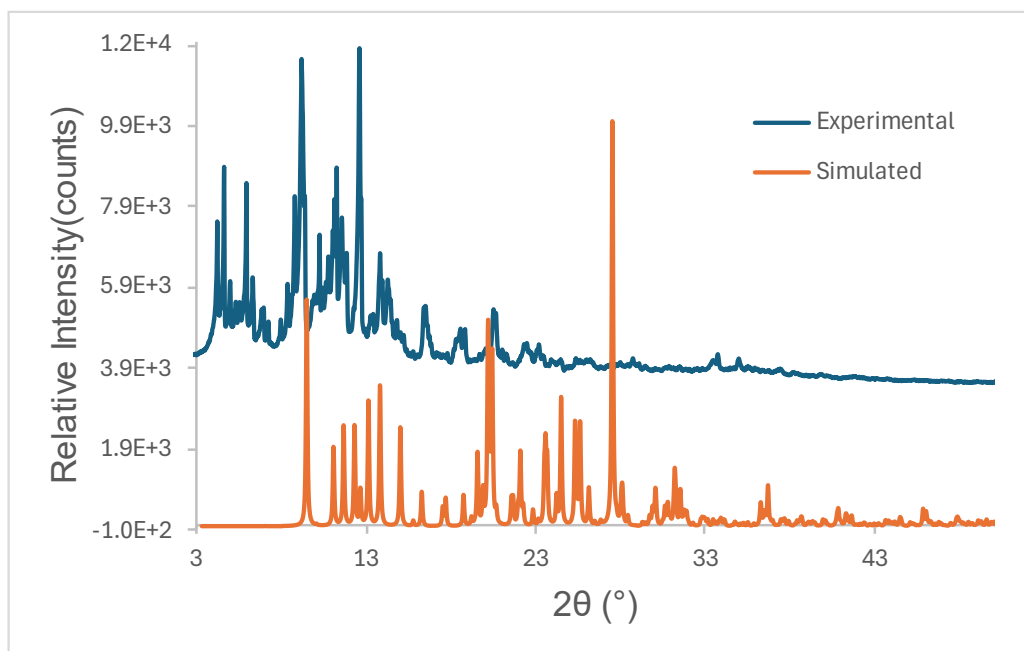


Figure S16. PXRD patterns of AnThio. The experimental pattern is the commercial source from the bottle and collected at -100°C , which shows both high and low temperature phases are present. The simulated pattern of AnThio from single crystal data collected at 300 K (27°C) is shown for comparison. The simulated pattern has been shifted by 0.32° degrees to align with experimental data.

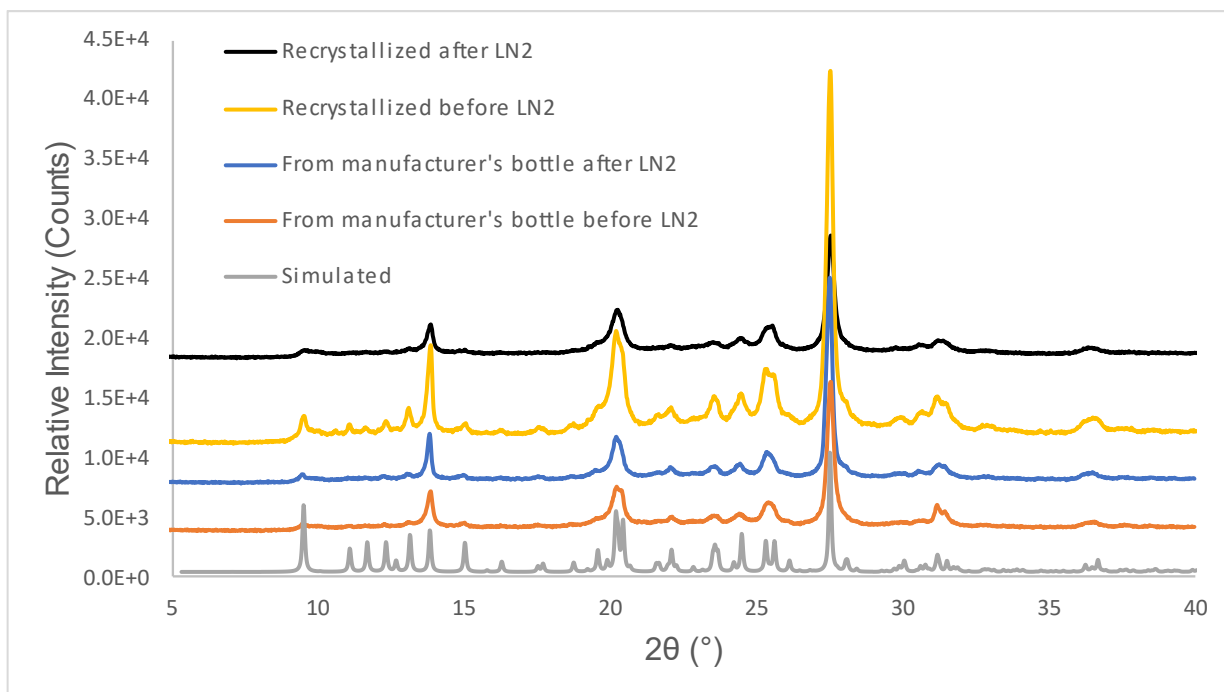


Figure S17. PXRD pattern of AnThio from manufacturer's bottle and recrystallized from ethyl acetate before and after ca. 5 min. exposure to liquid nitrogen. The simulated pattern has been shifted by 0.32° to align with experimental data.

9. Optical Microscopy with Variable-Temperature Stage

Videos of the thermosalience were recorded using a Leica DM2700 M microscope equipped with a Leica MC170 HD microscope camera. The temperature was controlled using a Linkam LTS420 variable temperature microscope stage with LNP96-S liquid nitrogen pump. Videos were taken while using a cooling rate of 5 K/min. The crystals used in these experiments were either directly from the manufacturer's bottle or recrystallized from ethyl acetate. The events happen between 180 and 160 K (-93 and -113 °C).

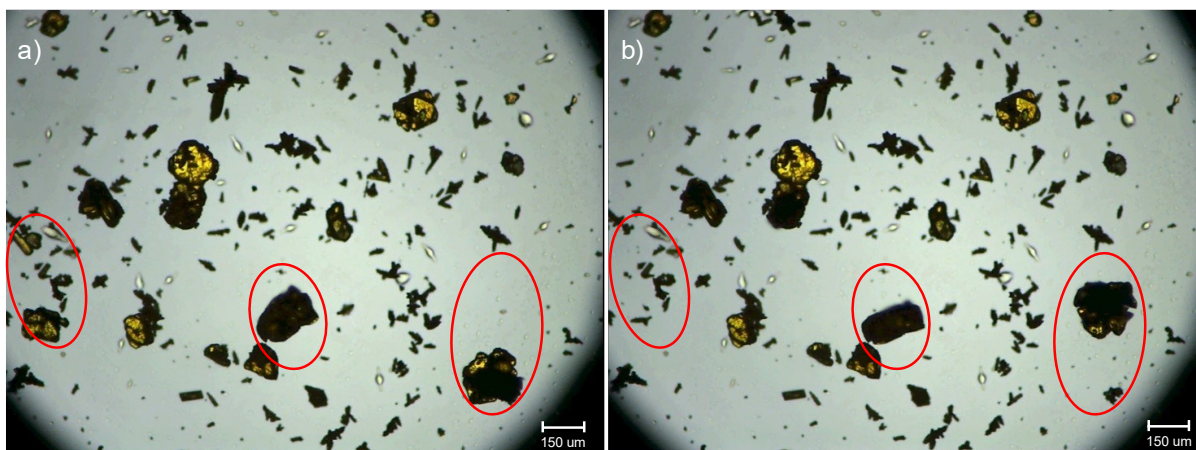


Figure S18. Optical microscope images of AnThio from the manufacturer's bottle directly a) before and b) after thermosalient event ca. 170 K (-103 °C) showing crystal movement. The large crystal on the left side leapt out of view. The images are taken from the supplementary video 1.

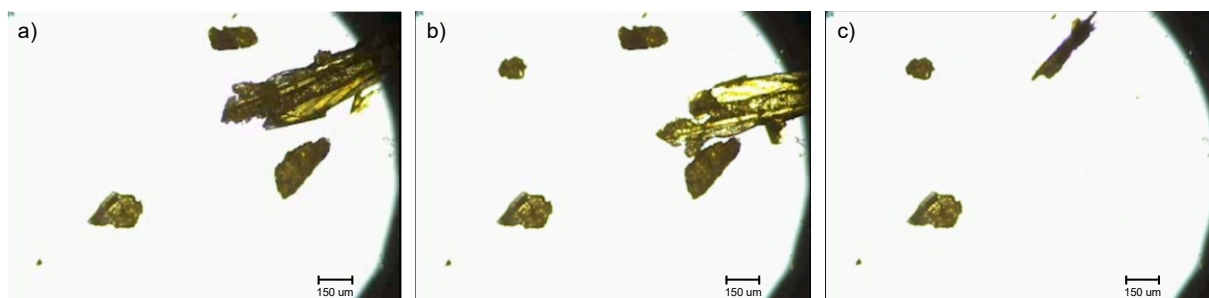


Figure S19. Optical microscope images of AnThio after recrystallization from ethyl acetate a) before, b) during, and c) after the thermosalient event around 170 K (-103 °C). The images are taken from supplementary video 2.

Supplementary Video 1: Video of AnThio from manufacturer's bottle exhibiting thermosalience upon cooling.

Supplementary Video 2: Video of AnThio recrystallized from ethyl acetate exhibiting thermosalience upon cooling.

10. References

1. G. C. George, III, K. M. Hutchins, *Chem. Eur. J.*, 2023, **29**, e202302482.
2. CrysAlis^{Pro} (2018) Oxford Diffraction Ltd.
3. SCALE3 ABSPACK (2005) Oxford Diffraction Ltd.
4. G. M. Sheldrick, *Acta Crystallogr., Sect. A: Found. Adv.* 2015, **A71**, 3-8.
5. G. M. Sheldrick, *Acta Crystallogr., Sect. C: Struct. Chem.* 2015, **C71**, 3-8.
6. O. V. Dolomanov, L. J. Bourhis, R. J. Gildea, J. A. K. Howard, H. Puschmann, *J. Appl. Cryst.* 2009, **42**, 339-341.
7. M. Lertkiatrakul, M. L. Evans, M. J. Cliffe, *J. Open Source Softw.* 2023, **8**, 5556-5559.